The photoelectron diffraction technique applied to advanced materials

2004 J. Phys.: Condens. Matter 16 S3441

(http://iopscience.iop.org/0953-8984/16/33/004)

INSTITUTE OF PHYSICS PUBLISHING JOURNAL OF PHYSICS: CONDENSED MATTER

J. Phys.: Condens. Matter **16** (2004) S3441–S3450 PII: S0953-8984(04)79889-6

The photoelectron diffraction technique applied to advanced materials

Antonio Tejeda[1] **and Enrique G Michel**

Departamento de Física de la Materia Condensada and Instituto Universitario de Ciencia de Materiales 'Nicolás Cabrera', Universidad Autónoma de Madrid, 28049 Madrid, Spain

Received 22 April 2004
Published 6 August 2004
Online at stacks.iop.org/JPhysCM/16/S3441
doi:10.1088/0953-8984/16/33/004

Abstract

The photoelectron diffraction method is a local structural technique related to angle resolved photoemission. Its chemical sensitivity allows one to study local environments, both at surfaces and in thicker layers; this leads to a large range of applications. The origin of photoelectron diffraction is the interference of the photoelectron that exits from the crystal directly and the waves multiply scattered in the lattice. The interference pattern detected provides structural information that depends on the kinetic energy of the photoelectron. This technique can be an extremely useful tool for studying the atomic structure of advanced materials. We will show how to obtain an atomic structure in the case of the (3×2) reconstruction of cubic silicon carbide.

(Some figures in this article are in colour only in the electronic version)

1. Introduction

The photoelectron diffraction (PED) technique is related to photoemission, the physical process where electrons in a material are extracted by radiation of sufficient energy. Photoelectron diffraction was first observed in 1970 by Siegbahn *et al* [1, 2] in a photoemission study on NaCl(100). They reported a larger core level intensity along the densely packed crystallographic planes [001] and [011]. They proposed a reasonable explanation, coherent with the experiments available at the time, based on the analogy of transmitted electrons with channelling processes. In transmission electron diffraction, the intensity increase is termed a Kikuchi band. Electrons that constitute these bands come out of the bulk material, and the width of their angular distribution is twice the Bragg angle corresponding to the set of planes that seems to give rise to them [3]. Later on, it was determined that the angular width of the PED maxima did not agree with the predictions for a Kikuchi band [3] and that the electrons

[1] Present address: Groupe de Physique des Solides, Université Paris 6 et 7, CNRS, UMR 75-88, 75251 Paris Cedex 05, France.

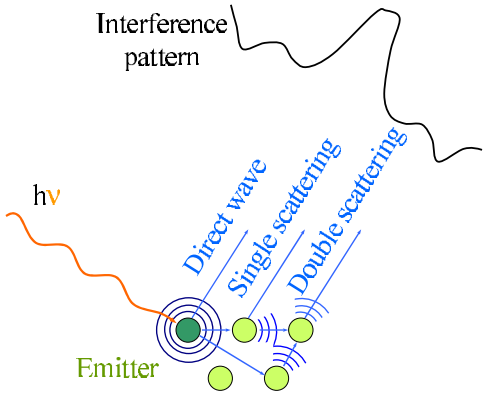

Figure 1. The photoelectron diffraction technique detects the interference of the photoelectron that exits the material with no dispersion and the multiply scattered waves. As the scattered waves interact with atoms in the neighbourhood of the emitter, the detected signal contains information on the local structure.

had a surface origin [4, 5]. Once the misunderstanding was corrected [4, 6, 7], the great potential of photoelectron diffraction was developed.

The origins of photoelectron diffraction are the dispersion processes of photoelectrons on their way out of the crystal. When an electron is photoexcited, the wave associated with the photoelectron can exit directly from the solid (wave Φ_0) or scatter on the atomic lattice (wave Φ_S). The interference of Φ_0 and Φ_S modifies the angular distribution of the intensity, leading to an enhanced emission along certain directions. As the scattered wave depends on the atomic environment of the emitter, the interference pattern contains information on the local structure (figure 1). The fundamentals of the PED formalism can be found in [8–10].

In the following, we present the general concepts of photoelectron diffraction and show that it can be an extremely useful tool for studying the atomic structure of advanced materials. In particular, we apply it to obtain the atomic structure of a Si-rich reconstruction of silicon carbide.

2. General concepts of photoelectron diffraction

2.1. Energy regimes

The photoelectron diffraction technique probes the atomic structure in the neighbourhood of a given emitter. On the other hand, photoemission can provide information on unlocalized electrons of the valence band or on localized electrons of core levels. Therefore, the most common way to obtain the local atomic structure by means of photoelectron diffraction is to study the atomic core levels, although there are other possibilities [11].

In the photoemission process under x-ray radiation, core level electrons are extracted, either in a standard way or via an Auger process. Depending on the origin of the detected electrons, photoelectron diffraction is called XPD (x-ray photoelectron diffraction) or AED (Auger electron diffraction). Both cases involve localized electrons but the mathematical description of XPD is more accurate. Auger electrons are not so easily described with spherical waves, as the process involves several states whose angular momenta are not always well defined. Anyway, under the assumption that multiple spherical harmonics are superposed, the outgoing electron waves can be considered approximately spherical [12] and the process is similar to XPD.

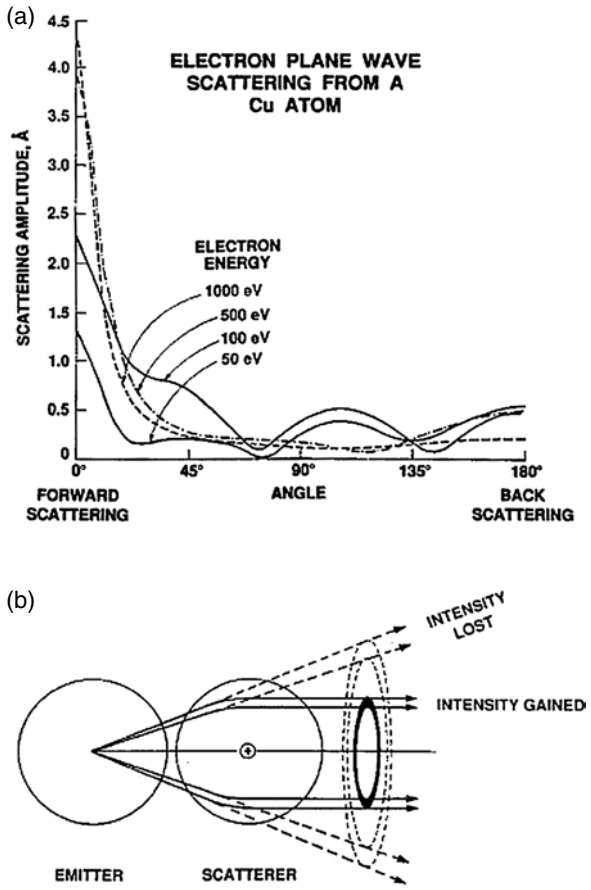

Figure 2. (a) The scattering amplitude for an electron plane wave incident on a Cu atom as a function of the angle and kinetic energy [15, 16]. (b) A diagram illustrating the forward scattering phenomenon. The atomic potential modifies the electron trajectory and the cylindrical symmetry produces an enhanced intensity along the direction between the emitter and scatterer [17].

The scattering of photoelectrons excited with x-ray radiation differs considerably depending on the kinetic energy range of the outgoing electron. For high kinetic energies (>500 eV), electrons have a scattering factor peaked in the direction between the emitter and scatterer (see figure 2(a)). These electrons experience a reduced number of scattering events on their way out of the solid. Therefore, the photoelectron diffraction maxima indicate directly the directions where the emitter has its first or second neighbours [12–14], as illustrated in figure 2(b). This situation is called the forward scattering regime. On the other hand, when the kinetic energy is less than a few hundred electronvolts, electrons have a more uniform scattering factor and they undergo multiple scatterings on their way out of the solid [18]. This situation is more difficult to interpret intuitively and simulation is often necessary to understand the data. In this case the structural information is contained subtly in the phase shift between the direct and the scattered waves. The scattering factor of this situation is characterized by the appearance of a pronounced maximum of the intensity that returns to the emitter, so it is sometimes called the backscattering regime. One of the areas of interest of these two regimes is that they allow one to determine bulk or surface structures using the same experimental set-up.

2.2. Comparison with other structural techniques

The photoelectron diffraction, low energy electron diffraction (LEED) and surface-extended x-ray absorption fine structure (SEXAFS) approaches are three techniques that rely on electron diffraction to obtain structural information. The photoelectron diffraction and SEXAFS ones are very similar, although the SEXAFS approach involves an angular integration of the signal [19]. Therefore, PED provides information on the bonding directions as well as on the bond lengths. There are more differences between LEED and PED. Photoelectron diffraction shows chemical sensitivity, which helps in the determination of the atomic environment of the different atoms in the structure. PED can also be used to determine bulk and surface structures in the same experiment. As it is sensitive to short range order around the emitter, it is possible to perform PED experiments when there is no LEED pattern [20]. However, LEED analysis is in general easier whenever a well-ordered structure with a single atomic species is considered.

3. Application to advanced materials

3.1. Introduction

Photoelectron diffraction has been successfully used to study several advanced materials. Many of its applications rely on its chemical sensitivity, that makes it particularly suitable for studying alloys [12], catalysis systems with several types of adatoms [21] and surfaces with adsorbed molecules [21–33]. Backscattering has been used to determine bond lengths [34, 35] and forward scattering to study interdiffusion or buried surfaces [36]. It is also possible to probe whether two atoms have the same atomic environment by comparing their diffraction patterns, without any further analysis [37]. When the data set is large and precise enough, PED can be used to determine a whole surface structure. This type of analysis is more scarce [10]. In the following, we describe the process of determining the whole surface structure of the (3×2) reconstruction of cubic SiC(001).

Silicon carbide is a IV–IV compound wide band-gap semiconductor with applications in high temperature, high power, high voltage and high frequency electronic devices and sensors [38–40]. The hexagonal (α) polytypes have the larger band gap (up to 3.3 eV) and are preferred for high temperature/high power devices. The cubic (β, also called 3C-SiC) polytype (band gap of 2.4 eV) is found to be more suitable for high frequency devices due to the higher carrier mobilities [38]. While different surface sensitive techniques have been applied to investigate the nature of the (3×2) reconstructions, there is almost no structural information on its atomic structure, besides the lateral atomic distribution as provided by scanning tunnelling microscopy (STM) [41], and a recent grazing incidence x-ray diffraction (GIXRD) study [42].

3.2. Experimental details

There are two basic configurations for photoelectron diffraction, depending on whether the detection angle or the photon energy is varied. When the photon energy is constant, photoelectrons are sampled in multiple solid angles over the sample. This can be done both at high ($>$500 eV) or low electron kinetic energies. Data are usually projected in two dimensions (see figure 3). The other experimental configuration is characterized by a fixed detection angle, while the photon energy is varied [23, 34]. Then, the backscattering effect is exploited. This configuration is particularly sensitive to the bond lengths of a given adsorption geometry [23, 29].

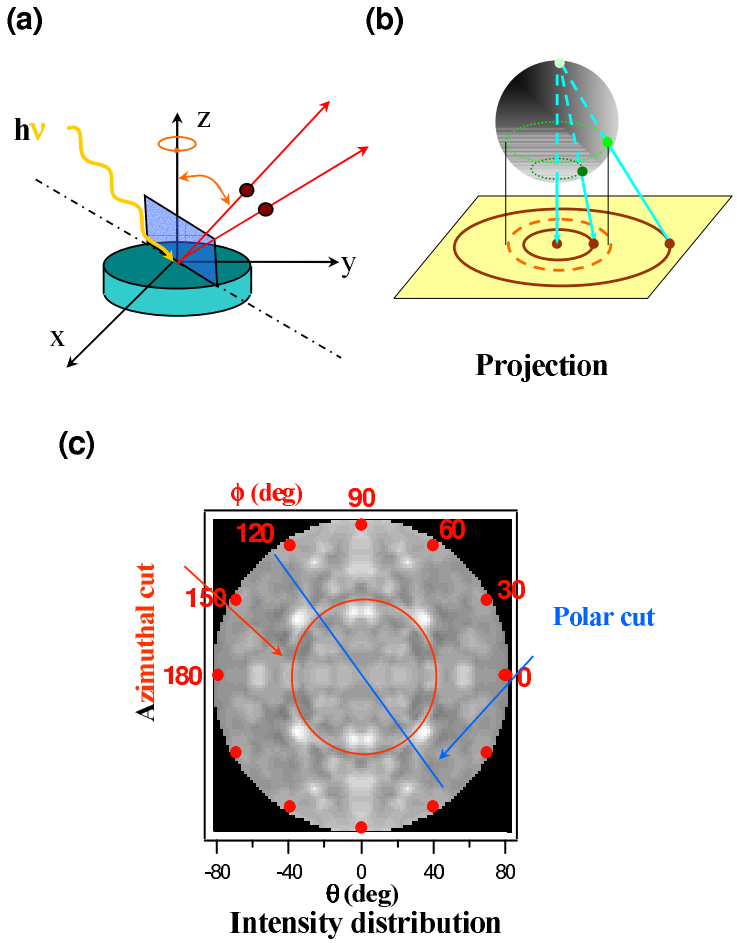

Figure 3. (a) The experimental set-up for photoelectron diffraction. Photoelectrons leaving the sample are detected along as many directions as possible, for a fixed photon energy. Alternatively, it is also possible to scan the photon energy for a fixed detection geometry. (b) The representation of photoelectron diffraction data in two dimensions is effected by projecting the detected intensity on a plane. (c) An example of detected intensity as a function of azimuthal and polar angles. The curves that have a constant polar (azimuthal) angle are known as azimuthal (polar) cuts.

We have performed studies using both high and low electron kinetic energies to determine the atomic structure of 3C-SiC(001)-(3×2), using synchrotron light from the 7.0.1 beamline of the Advanced Light Source. Experimental details [43, 44] and the preparation procedure [41] are described elsewhere.

3.3. Simulation details

Simulation of the photoelectron diffraction process allows one to obtain the maximum structural information about the material, although it is often very demanding in computational time. Considering only single-scattering processes and modelling photoelectrons as plane waves can considerably simplify the calculations, but certain physical situations will not be described adequately. We have used the EDAC code [45] conveniently adapted to the geometry of our

experimental set-up. It is based upon a spherical wave multiple-scattering cluster approach, where the surface is represented by a sufficiently large number of atoms surrounding the emitter. This code describes adequately the process of photoemission, the attenuation of the photoelectron in the solid, the thermal vibrations of the lattice, the refraction in the surface and the finite aperture of the analyser. The calculations have no further approximations besides those inherent to a muffin-tin construction.

3.4. Comparison between theory and experiment

The quality of the adjustment between theory and experiment is evaluated by means of a quantity called the *reliability factor (R-factor)*. The structural refinement process consists in the minimization of the *R*-factor versus the different structural parameters. For the photoelectron diffraction technique many *R*-factors have been defined, and there is no general consensus on which is the best one [46]. In this study we have used the *R*-factors defined by van Hove [47] and normalized by Saiki *et al* [48]. There are five types of these *R*-factors, but their weighted average favours the same structures as R_1 [49, 50], so we have basically employed the latter. The R_1-factor is defined as

$$R_1 = \frac{\sum_n |\chi^{\ddagger}_{\mathrm{exp}}(n) - \chi^{\ddagger}_{\mathrm{th}}|}{\sum_n |\chi^{\ddagger}_{\mathrm{exp}}(n)|} \tag{1}$$

where n corresponds to the channel of the azimuthal scan and $\chi^{\ddagger}_{\mathrm{exp}}$ and $\chi^{\ddagger}_{\mathrm{th}}$ are the experimental and theoretical normalized anisotropies, respectively [47, 48]. The anisotropy is the fast-varying part of the detected intensity, and it contains the information about the interference. The definition of $\chi\ddagger$ is

$$\chi\ddagger(\vec{k}) = \frac{I(\vec{k}) - I_0(\vec{k})}{I_0(\vec{k})} \tag{2}$$

where $\vec{k}$ is the photoelectron wavevector, $I(\vec{k})$ corresponds to the detected intensity without dependence on the photon flux and $I_0(\vec{k})$ is the smooth part of $I(\vec{k})$. The so-defined *R*-factor avoids an excess of influence of experimental noise at high polar angles and it compensates for the factor of 3–5 that there is between the theoretical and the experimental PED anisotropies, as also arises in LEED [10]. Once *R*-factors are defined, it is possible to determine the atomic structure, as we describe in the following.

3.5. Bulk structure

As a first step, we have monitored the C 1s and Si 2p photoemission peaks for a full hemispherical sector and 1253.6 eV photon energy. This is especially interesting in the case of a compound semiconductor, because photoelectrons from both Si and C atoms can be detected and used for the structural determination. It is also important in the case of a complex reconstruction like the (3×2) phase of SiC(001), that involves several Si layers. In this electron kinetic energy range, forward scattering dominates the spectra and, due to the large mean free path, the data are mainly sensitive to bulk atomic positions. A good agreement between theory and experiment was reached with only minor deformations of bulk atomic positions. Using the subsurface atomic positions found, we can now focus on the surface structure.

3.6. Model discrimination

As second step, the bulk atomic positions so determined have been used to construct a series of clusters that reproduce the different structural models put forward in the literature [41, 42, 51–56]. These models include the ADRM (alternate dimer row model) (2×3) [55]; the ADRM

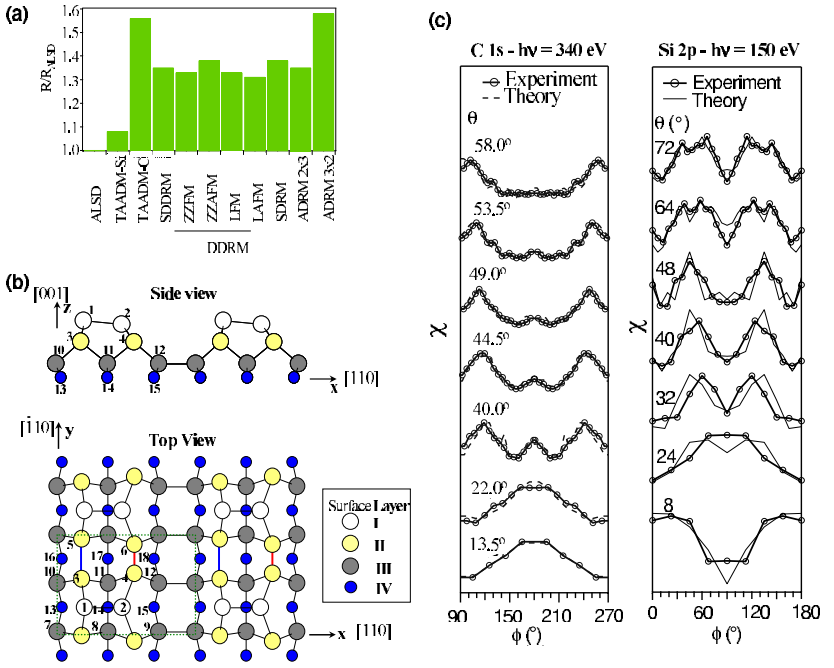

Figure 4. (a) The *R*-factors of the different models relative to the *R*-factor of the ALSD model. The TAADM-ALSD model is the most favoured one. (b) Atomic positions in the TAADM-ALSD model. (c) Comparison between experimental and simulated azimuthal anisotropy curves for C 1s and Si 2p for the refined model.

(3 × 2) [41]; the SDRM (single-dimer-row model); the SDDRM (symmetric double-dimer-row model) [52]; the ZZAFM-DDRM (zigzag antiferromagnetic DDRM) [56]; the ZZFM-DDRM (zigzag ferromagnetic DDRM) [56]; the LAFM-DDRM (layered antiferromagnetic DDRM) [56]; the LFM-DDRM (layered ferromagnetic DDRM) [56]; the TAADM (two-adlayer asymmetric dimer model) [56]; the TAADM-Si and TAADM-C models which are modifications of the TAADM model [44]; and the alternating short and long dimer model (ALSD) [42], a modified version of the TAADM-Si.

The clusters have been used to model the experimental anisotropy curves. Low energy data are sensitive to the structure of the topmost surface layers. They allow us to distinguish between the different models [57]. We do not expect a perfect agreement between experiment and simulation, because this would require a detailed model refinement. However, models that present a poor agreement with experiment can be safely discarded without further tests, because minor modifications of the atomic positions are not able to convert the situation to a good agreement. Figure 4(a) shows the ratios between the mean *R*-factors of the different models and that of the ALSD model. The details of the analysis are presented elsewhere [43, 44]. ALSD-TAADM models are considerably better than the rest of the models proposed in the literature, so only these models will be considered in the following.

3.7. Model refinement

A more detailed analysis of low kinetic energy data allows us to refine the atomic structure of the TAADM-ALSD model (see figure 4(b)). The refinement consists in the determination of the global minima in a multidimensional hypersurface. The main difficulty of this process is the

large number of structural parameters, especially in large unit cells. The number of parameters can be reduced by application of the symmetry properties or other available information on the surface (chemical composition, lateral periodicity, or in the case of adsorbed atoms, the nature of the adsorption site). In the case of the (3×2) reconstruction, we have varied the positions of all atoms in the first three layers of the cluster, without symmetry breaking. The number of parameters varied was 14: 11 structural parameters (x_1, z_1, x_2, z_2, x_3, y_3, z_3, x_4, y_4, z_4, and the vertical coordinate of the third layer z(III); see figure 4(b)) and three non-structural parameters (the interstitial potential among atoms, the surface position and the electron mean free path). As the total number of experimental points was 375, this gives a ratio of $\sim$27 experimental points per parameter.

In the simplest situation, all parameters are independent of each other and each one can be optimized separately. However, this case is not probable in cartesian coordinates. In the commonest situation the parameters are correlated, and furthermore they are mixed in the diffraction process. Thus, it is necessary to adjust them simultaneously [46]. The search efficiency depends on the number of parameters considered, the variation range and the step employed for each parameter. With small steps, the precision is enhanced, except when steps are so small ($\sim$0.01 Å) [58] that they detect the noise of the R-factor topology.

In general, some parameters are varied while others are kept constant, until all of them have been progressively varied and several iterations have been performed. The parameters most sensitive to R-factor variations must be varied first [59]. It is convenient to proceed in this way, especially in the first refinement stages, to prevent the less sensitive parameters from reaching unphysical values, in order to compensate displacements of the more sensitive coordinates. Normally, coordinates perpendicular to the surface affect the R-factor more than parallel ones [46], because the transferred moment has its largest component perpendicular to the surface. Also surface coordinates influence the R-factor more than bulk ones, due to the electron attenuation. In consequence, the standard procedure consists in first varying the perpendicular coordinates of surface atoms, and then varying the coordinates associated with deeper atoms.

In the refinement process, a series of local minima can be observed, which it is mandatory to avoid. The aleatory minima of the R-factor usually have values near the average, while those originated by diffraction coincidences are deeper [60]. In order to detect these local minima, the physical meaning of the parameter values should be verified. The contrast between local and global minima can also be increased by a better description of the dispersion potential, with a higher number of phase shifts [61]. Another possibility is to consider different R-factors, because when the absolute minimum is obtained, every R-factor reaches a minimum for the same parameters. In contrast, local minima correspond to different positions with the different R-factors [62].

In the example of the (3×2) reconstruction of silicon carbide, the surface structural parameters were systematically modified until an absolute minimum in the R-factor was found. A selection of the corresponding experimental and theoretical curves for the best model found is shown in figure 4(c). The optimal structure was reached for an asymmetric dimer with a difference in height of 0.25 Å. Each atom of the dimer is bonded to two other Si atoms which dimerize as well. The bonding length of this second-layer dimers varies depending on whether they are bonded to the upper or lower atom of the first-layer dimer.

4. Conclusions

We summarized the general concepts of the photoelectron diffraction technique including its physical origin, which allowed us to explain several of the features of this technique, such

as its chemical sensitivity, its angular resolution and the possibility of studying both surface and bulk structures. The use of *R*-factors is the most powerful tool for comparing theory and experiment and for determining atomic structures. We employ this technique to study a Si-rich surface of silicon carbide, a wide band-gap semiconductor with many technological applications. This example shows how photoelectron diffraction can be used to distinguish among all the models available in the literature and to determine the atomic positions of the correct model.

Acknowledgments

This work was supported in part by CAM (Spain) (07N/0022/2002 and FPI grant of A Tejeda). The synchrotron radiation experiments performed at the ALS (Berkeley) were supported by the Northern Illinois University Graduate School Funds and by NSF. We thank P Soukiassian for the collaboration that made possible the study of silicon carbide reconstructions and F García de Abajo for providing us with the multiple-scattering code and for helpful discussions. The authors are grateful also to D Dunham, E Rotenberg and J Denlinger, who participated in the experiments on the silicon carbide surfaces. The expert and outstanding technical assistance of the ALS staff is gratefully recognized.

References

[1] Siegbahn K, Gelius U, Siegbahn H and Olson E 1970 *Phys. Lett.* A **32** 221
[2] Siegbahn K, Gelius U, Siegbahn H and Olson E 1970 *Phys. Scr.* **1** 272
[3] Baird R J, Fadley C S and Wagner L F 1977 *Phys. Rev.* B **15** 666
[4] Egelhoff W F 1985 *J. Vac. Sci. Technol.* A **3** 1511
[5] Egelhoff W F 1997 *Phys. Rev. Lett.* **59** 559
[6] Egelhoff W F 1984 *J. Vac. Sci. Technol.* A **2** 350
[7] Armstrong R A and Egelhoff W F 1985 *Surf. Sci.* **154** L225
[8] Barton J J, Robey S W and Shirley D A 1986 *Phys. Rev.* B **34** 778
[9] Fritzsche V 1992 *Surf. Sci.* **265** 187
[10] Fadley C S 1993 *Surf. Sci. Rep.* **19** 231
[11] Osterwalder J, Greber T, Stuck A and Schlapbach L 1990 *Phys. Rev. Lett.* **64** 2683
[12] Egelhoff W F 1990 *Crit. Rev. Solid State Mater. Sci.* **16** 213
[13] Osterwalder J, Aebi P, Fasel R, Naumovic D, Schwaller P, Kreutz T, Schlapbach L, Abukawa T and Kono S 1995 *Surf. Sci.* **331–333** 1002
[14] Osterwalder J, Greber T, Wetli E, Wider J and Neff H J 2000 *Prog. Surf. Sci.* **64** 65
[15] Fink M and Ingram J 1972 *At. Data* **4** 1
[16] Webb M B and Lagally M G 1973 *Solid State Phys.* **28** 301
[17] Tong S Y, Puga M W, Poon H C and Xu M L 1986 *Chemistry and Physics of Solid Surfaces* vol 6, ed R Vanselow and R Howe (Berlin: Springer) p 509
[18] Fadley C S *et al* 1997 *Surf. Rev. Lett.* **4** 421
[19] Pendry J B 1974 *Low Energy Electron Diffraction* (London: Academic)
[20] Aebi P *et al* 1998 *Surf. Sci.* **402–404** 614
[21] Schindler K M, Fritzsche V, Asensio M C, Gardner P, Ricken D E, Robinson A W, Bradshaw A M, Woodruff D P, Conesa J C and González-Elipe A R 1992 *Phys. Rev.* B **46** 4836
[22] Schindler K M, Hofmann Ph, Fritzsche V, Bao S, Kulkarni S, Bradshaw A M and Woodruff D P 1993 *Phys. Rev. Lett.* **71** 2054
[23] Woodruff D P and Bradshaw A M 1994 *Rep. Prog. Phys.* **57** 1029
[24] Petersson L G, Kono S, Hall N F T, Fadley C S and Pendry J B 1979 *Phys. Rev. Lett.* **42** 1545
[25] Fadley C S, Kono S, Petersson L G, Goldberg S M, Hall N F T, Lloyd J T and Hussain Z 1979 *Surf. Sci.* **89** 52
[26] Wesner D A, Coenen F P and Bonzel H P 1989 *Phys. Rev.* B **39** 10770
[27] Wesner D A, Coenen F P and Bonzel H P 1986 *Phys. Rev.* B **33** 8837
[28] Wesner D A, Coenen F P and Bonzel H P 1988 *Phys. Rev. Lett.* **60** 1045
[29] Kittel M *et al* 2001 *Surf. Sci.* **470** 311

[30] Fasel R, Aebi P, Agostino R G, Naumovic D, Osterwalder J, Santianello A and Schlapbach L 1996 *Phys. Rev. Lett.* **76** 4733
[31] Booth N A *et al* 1997 *Surf. Sci.* **387** 152
[32] Bengió S *et al* 2002 *Phys. Rev.* B **66** 195322
[33] Franco N, Avila J, Davila M E, Asensio M C, Woodruff D P, Schaff O, Fernandez V, Schindler K M, Fritzsche V and Bradshaw A M 1997 *Phys. Rev. Lett.* **79** 673
[34] Greber T, Wider J, Wetli E and Osterwalder J 1998 *Phys. Rev. Lett.* **81** 1654
[35] Fasel R, Aebi P, Osterwalder J and Schlapbach L 1995 *Surf. Sci.* **331–333** 80
[36] Saiki R S, Kaduwela A P, Osterwalder J, Fadley C S and Brundle C R 1989 *Phys. Rev.* B **40** 1586
[37] Osterwalder J, Aebi P, Schwaller P, Schlapbach L, Shimoda M, Mochiku T and Kadowaki K 1994 *Appl. Phys.* A **60** 247
[38] Matsunami H M and Pensl G 1998 *Silicon Carbide, A Review of Fundamental Questions and Applications to Current Device Technology* vol 1 & 2, ed W J Choyke (Berlin: Akademie) and references therein
[39] Capano M A and Trew R (ed) 1997 Silicon carbide electronic devices and materials *Mater. Res. Soc. Bull.* **22** and references therein
[40] 1999 *IEEE Trans. Electron Devices* **46** (special issue on Silicon Carbide Electronic Devices) and references therein
[41] Semond F, Soukiassian P, Mayne A, Dujardin G, Douillard L and Jaussaud C 1996 *Phys. Rev. Lett.* **77** 2013
[42] D'angelo M, Enriquez H, Aristov V Yu, Soukiassian P, Renaud G, Barbier A, Noblet M, Chiang S and Semond F 2003 *Phys. Rev.* B **68** 165321
[43] Tejeda A, Michel E G, Dunham D, Soukiassian P, Denlinger J D, Rotenberg E, Hurych Z D and Tonner B 2003 *Mater. Sci. Forum* **433** 579
[44] Tejeda A, Dunham D, García de Abajo F J, Denlinger J D, Rotenberg E, Michel E G and Soukiassian P 2004 *Phys. Rev.* B at press
[45] García de Abajo F J, Van Hove M A and Fadley C S 2001 *Phys. Rev.* B **63** 075404 See also EDAC code at http://electron.lbl.gov/∼edac and http://dipc.ehu.es/edac
[46] Van Hove M A, Moritz W, Over H, Rous P J, Wander A, Barbieri A, Materer N, Starke U and Somorjai G A 1993 *Surf. Sci. Rep.* **19** 191
[47] Van Hove M A, Tong S Y and Elconin M H 1977 *Surf. Sci.* **64** 85
[48] Saiki R S, Kaduwela A P, Sagurton M, Osterwalder J, Friedman D J, Fadley C S and Brundle C R 1993 *Surf. Sci.* **282** 33
[49] Saiki R S, Kaduwela A P, Kim Y J, Friedman D J, Osterwalder J, Thevuthasan S and Fadley C S 1992 *Surf. Sci.* **279** 305
[50] Bullock E L, Herman G S, Yamada M, Friedman D J and Fadley C S 1990 *Phys. Rev.* B **41** 1703
[51] Dayan M 1985 *J. Vac. Sci. Technol.* A **3** 361
[52] Dayan M 1986 *J. Vac. Sci. Technol.* A **4** 38
[53] Hara S, Slijkerman W F J, van der Veen J F, Ohdomari I, Misawa S, Sakuma E and Yoshida S 1990 *Surf. Sci. Lett.* **231** L196
[54] Hara S, Misawa S, Yoshida S and Aoyagi Y 1994 *Phys. Rev.* B **50** 4548
[55] Yan H, Smith A P and Jónsson H 1995 *Surf. Sci.* **330** 265
[56] Lu W, Krüger P and Pollmann J 1999 *Phys. Rev.* B **60** 2495
[57] Fasel R, Aebi P, Osterwalder J, Schlapbach L, Agostino R G and Chiarello G 1994 *Phys. Rev.* B **50** 14516
[58] Rous P J 1992 *Prog. Surf. Sci.* **39** 3
[59] Adams D L, Jensen V, Sun X F and Vollesen J H 1988 *Phys. Rev.* B **38** 7913
[60] Rous P J 1993 *Surf. Sci.* **296** 358
[61] Adams D L, Nielsen H B and Van Hove M A 1979 *Phys. Rev.* B **20** 4789
[62] Van Hove M A and Koestner R J 1984 *Determination of Surface Structure by LEED* ed P M Marcus and F Jona (New York: Plenum)